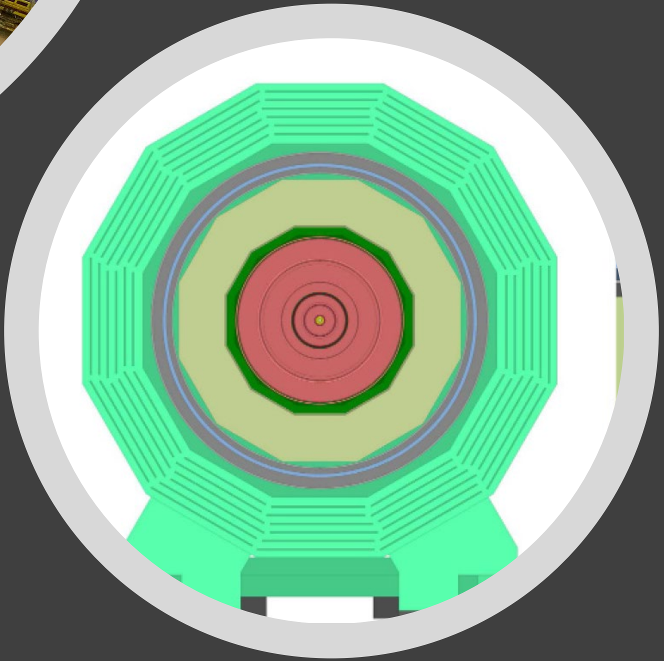

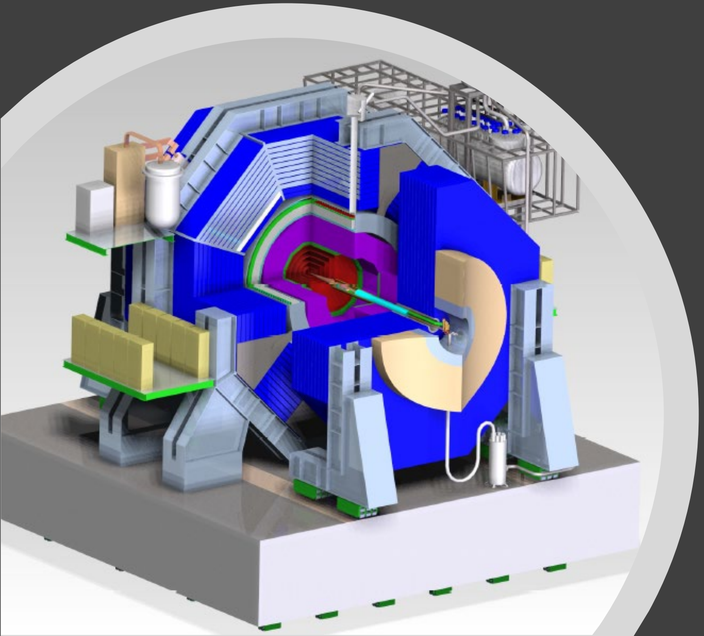

Design a flavour-physics detector for FCC-ee

Sarah Eno, U. Maryland

FNAL FCC “fun” event

12 Oct 2022

schedule

- 7 minute presentation by Sarah
- 15 minutes brain storming in groups
- 10 minutes discussion of group results

disclaimer

Obviously, you cannot design a billion-dollar detector in a 20-minute BS session. This “exercise” is aimed to get people talking in fun way.

This is a safe space, so don’t be afraid to be wrong. Senior people (including Sarah Eno)
should refrain from castigating people who make “wrong” statements about their favorite detectors.
I’m not expert at much of this, so there are probably wrong statements in these slides. Buyer beware.

Future detectors

Lots of fascinating work has been done designing detectors for the ILC. Strong work has been done on “strawman” detectors for FCC-ee, FCC-hh, C^3, CLIC, the muon detector, and CEPC. (okay, here I’m trying to list every possible currently designed guess at a future detector… will stop doing that).

Much of that work has concentrated on
- Precision measurements of Higgs properties
- Energy frontier physics at TeV scale electron-positron colliders (measurement of properties of SUSY particles, etc)

However the US has a long history of impact in flavour physics, especially b physics.

CESR on the campus of Cornell University in Ithaca, New York.

The BaBar Experiment

Welcome to the BABAR public web site. BABAR is a particle physics experiment designed to study some of the most fundamental questions about the universe by exploring its basic constituents - elementary particles. The BABAR Collaboration's research topics include the nature of antimatter, the properties and interactions of the particles known as quarks and leptons, and searches for new physics. We invite you to explore the site and learn about the BABAR detector, our research, and the physicists who perform it.

Flavour physics now

Report of the Frontier for Rare Processes and Precision Meaurements: arXiv:2210.04765

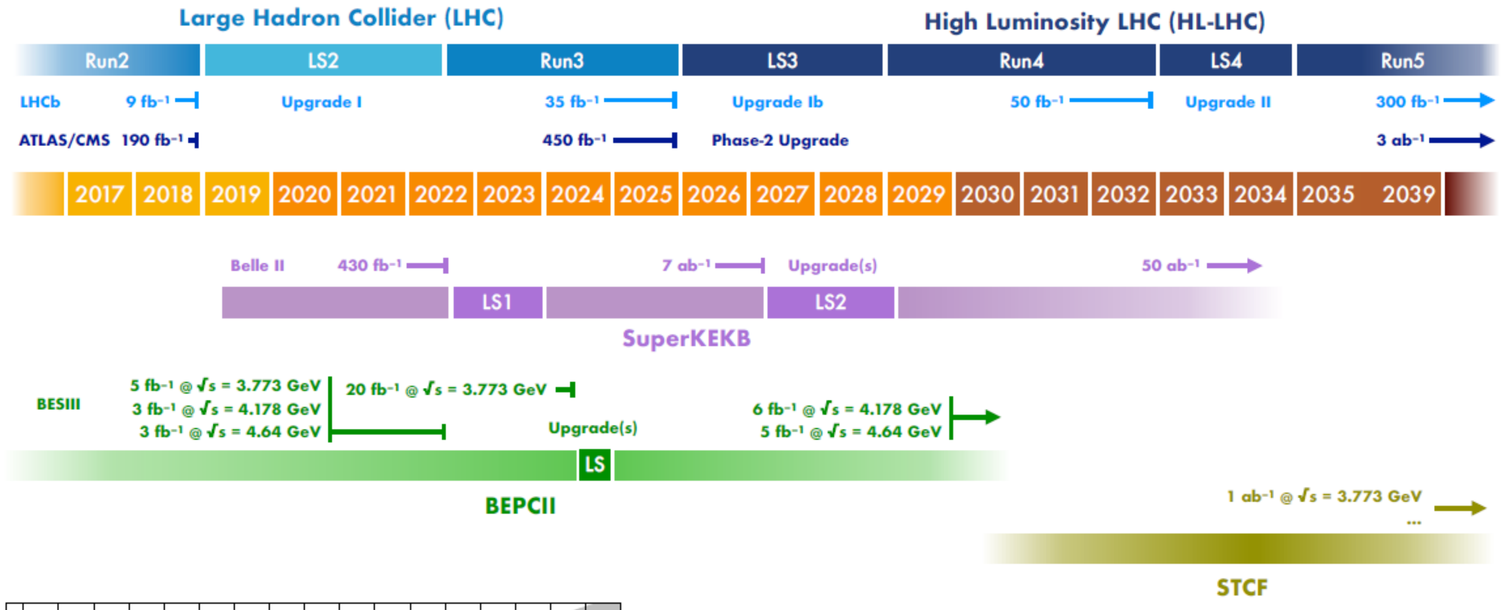

B physics now dominated by Japan and CERN. Some US participation in LHCb and in Belle-2. c and tau studied in China.

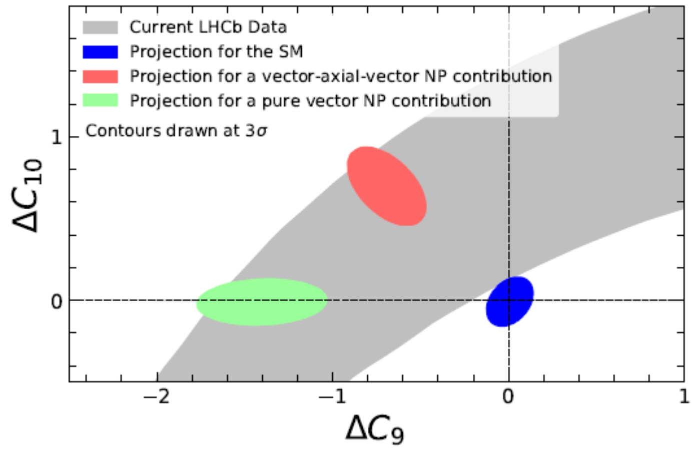

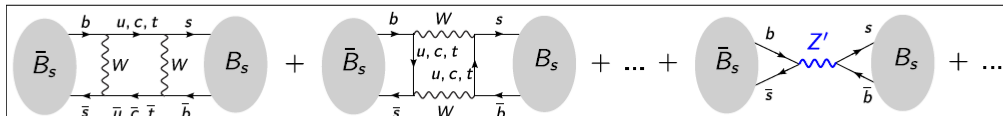

Studies of rare b decays have historically been sensitive to models with new particles. The heaviness of the top was first sensed through neutral b oscillations. CP violation is of course a key interest. Right now there are several observed anomalies in b decay

B physics now

Weak Decays of b and c quarks: report of topical group RF1 https://arxiv.org/abs/2208.05403

Observable	Current best	Belle II $50\,\text{ab}^{-1}$	Belle II $250\,\text{ab}^{-1}$	LHCb $50\,\text{fb}^{-1}$	LHCb $300\,\text{fb}^{-1}$	ATLAS $3\,\text{ab}^{-1}$	CMS $3\,\text{ab}^{-1}$	BESIII $20\,\text{fb}^{-1}$ (∗)	STCF $1\,\text{ab}^{-1}$ (∗)
Lepton-flavor-universality tests									
$R_K(1 < q^2 < 6\,\text{GeV}^2/c^4)$	0.044 [49]	0.036	0.016	0.017	0.007				
$R_{K^*}(1 < q^2 < 6\,\text{GeV}^2/c^4)$	0.12 [50]	0.032	0.014	0.022	0.009				
$R(D)$	0.037 [51]	0.008	< 0.003	na	na				
$R(D^*)$	0.018 [51]	0.0045	< 0.003	0.005	0.002				
Rare decays									
$\mathcal{B}(B_s^0 \to \mu^+\mu^-)$ $[10^{-9}]$	0.46 [52, 53]			na	0.16	0.46–0.55	0.39		
$\mathcal{B}(B^0 \to \mu^+\mu^-)/\mathcal{B}(B_s^0 \to \mu^+\mu^-)$	0.69 [52, 53]			0.27	0.11	na	0.21		
$\mathcal{B}(B^0 \to K^{*0}\tau^+\tau^-)$ UL $[10^{-3}]$	2.0 [54, 55]	0.5	na						
$\mathcal{B}/\mathcal{B}_{\text{SM}}(B^+ \to K^+\nu\overline{\nu})$	1.4 [56, 57]	0.08–0.11	na						
$\mathcal{B}(B \to X_s\gamma)$	10% [58, 59]	2–4%	na						
CKM tests and *CP* violation									
α	5° [60]	0.6°	0.3°						
$\sin 2\beta(B^0 \to J/\psi K_S^0)$	0.029 [61]	0.005	0.002	0.006	0.003				
γ	4° [62]	1.5°	0.8°	1°	0.35°			0.4° (†)	$< 0.1°$ (†)
$\phi_s(B_s^0 \to J/\psi\,\phi)$	32 mrad [63]			10 mrad	4 mrad	4–9 mrad	5–6 mrad		
$\lvert V_{ub}\rvert(B^0 \to \pi^-\ell^+\nu)$	5% [64, 65]	2%	$< 1\%$	na	na				
$\lvert V_{ub}\rvert/\lvert V_{cb}\rvert(\Lambda_b^0 \to p\mu^-\overline{\nu})$	6% [66]			2%	1%				
$f_{D^+}\lvert V_{cd}\rvert(D^+ \to \mu^+\nu)$	2.6% [67]	1.4%	na					1.0%	0.15%
$S_{CP}(B^0 \to \eta' K_S^0)$	0.08 [68, 69]	0.015	0.007	na	na				
$A_{CP}(B^0 \to K_S^0\pi^0)$	0.15 [68, 70]	0.025	0.018	na	na				
$A_{CP}(D^+ \to \pi^+\pi^0)$	11×10^{-3} [71]	1.7×10^{-3}	na	na	na			na	na
$\Delta x(D^0 \to K_S^0\pi^+\pi^-)$	18×10^{-5} [72]	na	na	4.1×10^{-5}	1.6×10^{-5}				
$A_\Gamma(D^0 \to K^+K^-, \pi^+\pi^-)$	11×10^{-5} [73]	na	na	3.2×10^{-5}	1.2×10^{-5}				

Table 1: Projected uncertainties (or 90% CL upper limits) in several key heavy-flavor observables over the next two decades. A missing entry means that the observable cannot be measured, the abbreviation na means that, although the observable can be measured, the projected uncertainty is not available. Projections are taken from Refs. [28, 30, 74] (Belle II), Refs. [45, 75] (LHCb), Ref. [37] (ATLAS and CMS), Refs. [34, 48] (BESIII and STCF). (∗) Integrated luminosity at $\sqrt{s} = 3.773$. (†) Projected uncertainties on γ resulting from BESIII/STCF measurements of the D strong-phase differences, which will contribute as external inputs to the Belle II and LHCb measurements.

FUTURE CIRCULAR COLLIDER future

In the future, at circular electron-positron colliders, such as FCC-ee and CEPC, there will be a tera-Z run. One of the interesting physics possibilities of that run is improving our understanding of flavor physics via precision studies of the b quark and tau lepton.

Particle production (10^9)	$B^0/\overline{B}^0$	B^+/B^-	$B^0_s/\overline{B}^0_s$	$B^+_c/\overline{B}^-_c$	$\Lambda_b/\overline{\Lambda}_b$	$c\overline{c}$	$\tau^+\tau^-$
Belle II	27.5	27.5	n/a	n/a	n/a	65	45
FCC-ee	620	620	150	4	130	600	170

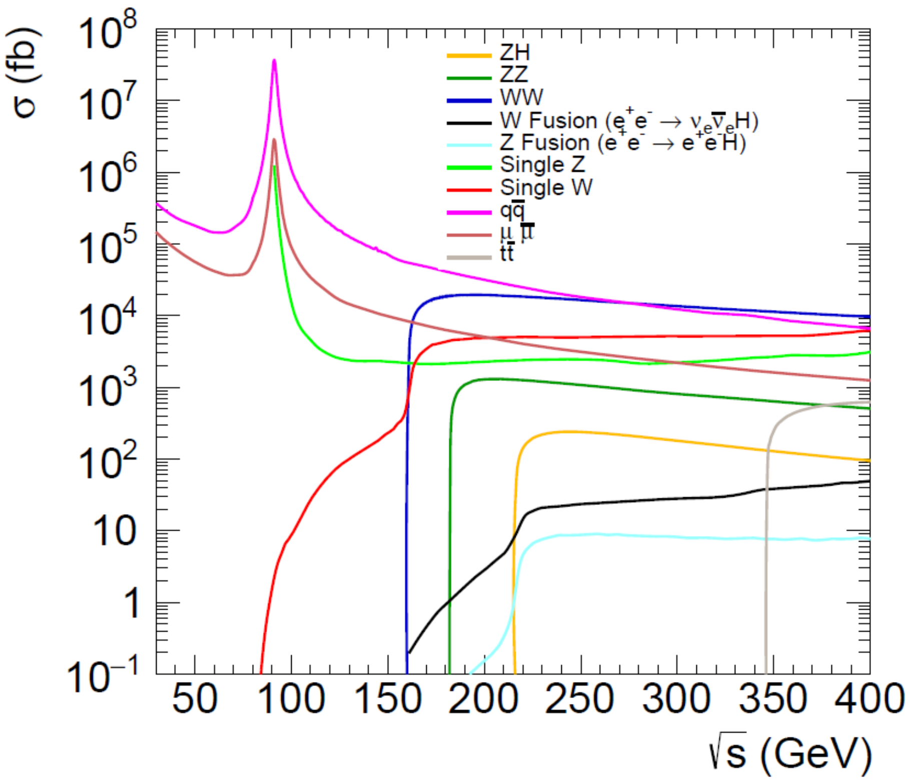

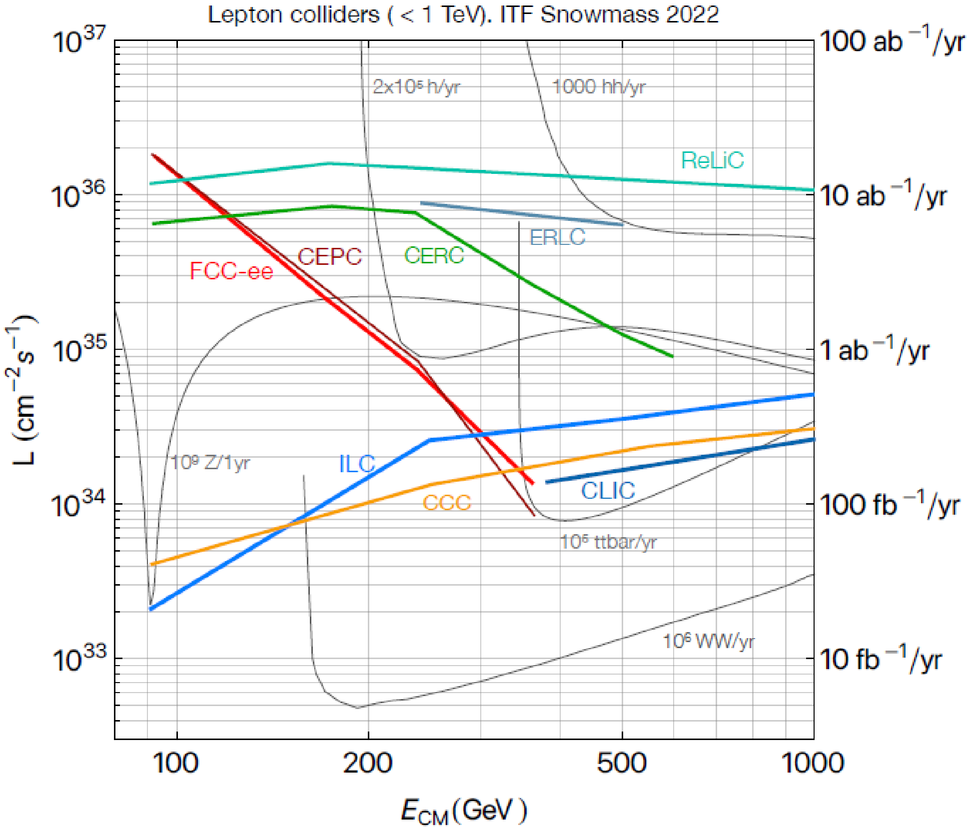

There will be four interaction regions in such a collider. One could be a detector optimized for flavour physics (like LHCb and ALICE at LHC).

Currently, not much real thought into designing a detector optimized for flavour physics (there is a nice paper from CEPC).

Shall we have fun thinking about which of the current detectors would be the best for flavour physics? Or is there need for a new design?

Some current proposed detectors

ILC SiD experiment

Figure II-1.1
SiD on its platform, showing tracking (red), ECAL (green), HCAL (violet) and flux return (blue).

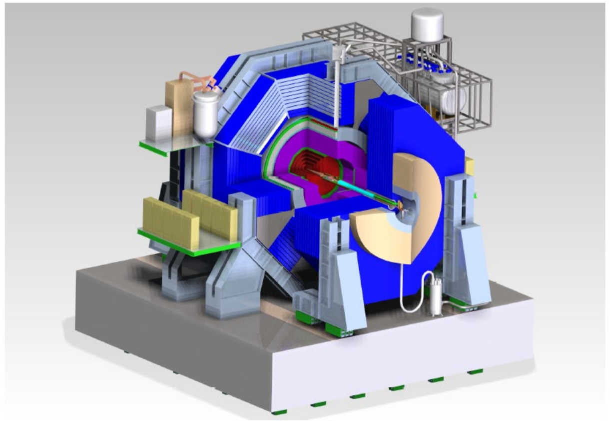

FCC-ee “strawman” Higgs factory experiment

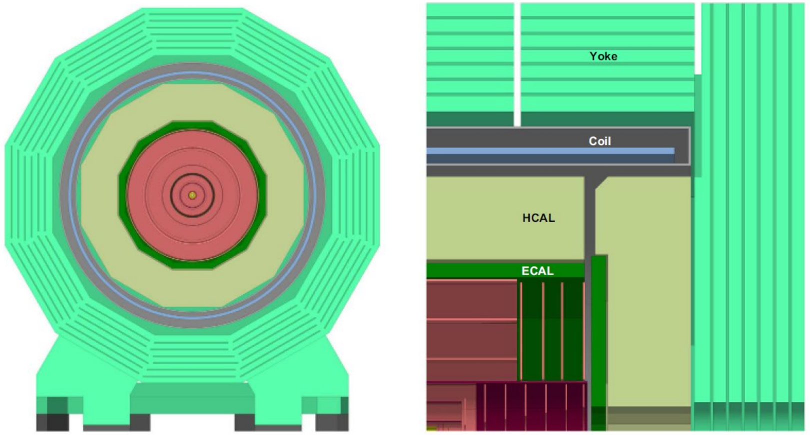

Fig. 7.4. The CLD concept detector: end view cut through (left), longitudinal cross section of the top right quadrant (right).

Nice detectors, but may not be optimal for flavour physics

ILC ILD experiment

Figure III-1.1
View of the ILD detector concept.

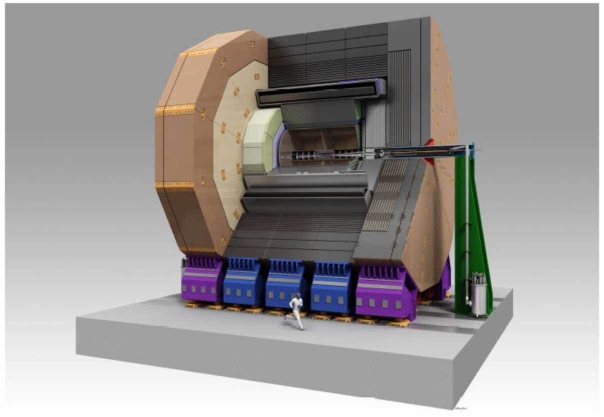

IDEA dual readout (precision ECAL version)

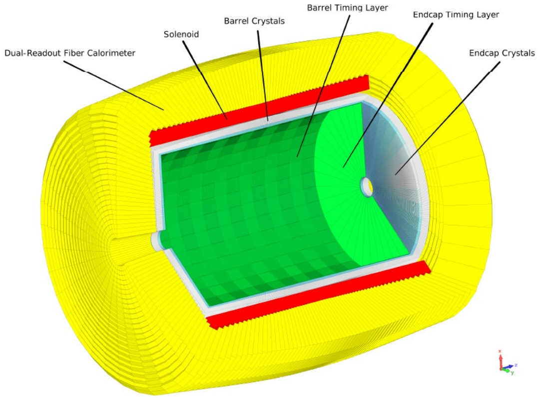

Higgs factory canonical specs

Optimization criteria commonly used for Higgs factor experiments

Physics process	Measurands	Detector subsystem	Performance requirement
$ZH, Z \to e^+e^-, \mu^+\mu^-$ $H \to \mu^+\mu^-$	$m_H, \sigma(ZH)$ $\mathrm{BR}(H \to \mu^+\mu^-)$	Tracker	$\Delta(1/p_T) =$ $2 \times 10^{-5} \oplus \frac{0.001}{p(\mathrm{GeV}) \sin^{3/2}\theta}$
$H \to b\bar{b}/c\bar{c}/gg$	$\mathrm{BR}(H \to b\bar{b}/c\bar{c}/gg)$	Vertex	$\sigma_{r\phi} =$ $5 \oplus \frac{10}{p(\mathrm{GeV}) \times \sin^{3/2}\theta} (\mu\mathrm{m})$
$H \to q\bar{q}, WW^*, ZZ^*$	$\mathrm{BR}(H \to q\bar{q}, WW^*, ZZ^*)$	ECAL HCAL	$\sigma_E^{\mathrm{jet}}/E =$ $3 \sim 4\%$ at 100 GeV
$H \to \gamma\gamma$	$\mathrm{BR}(H \to \gamma\gamma)$	ECAL	$\Delta E/E =$ $\frac{0.20}{\sqrt{E(\mathrm{GeV})}} \oplus 0.01$

Compared to b physics, lots of emphasis on jet resolutions and performance at high pT.
Not much need for meson identificatoin

Current state-of-the-art flavour experiments

Belle-2:

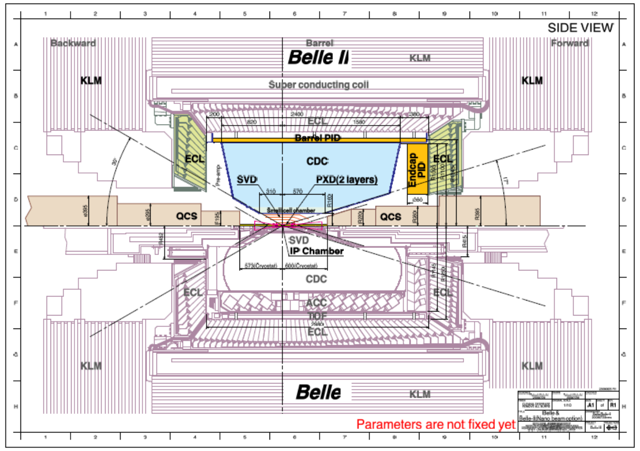

Figure 1.9: Upgraded Belle II spectrometer (top half) as compared to the present Belle detector (bottom half).

Emphasis on particle (even hadron) identification
- K/pi
- p/pi
- etc

Tracks tend to be lower-momentum, so best to minimize multiple scattering

Need excellent b tagging-> pixel detector

Not much need for jet reconstruction

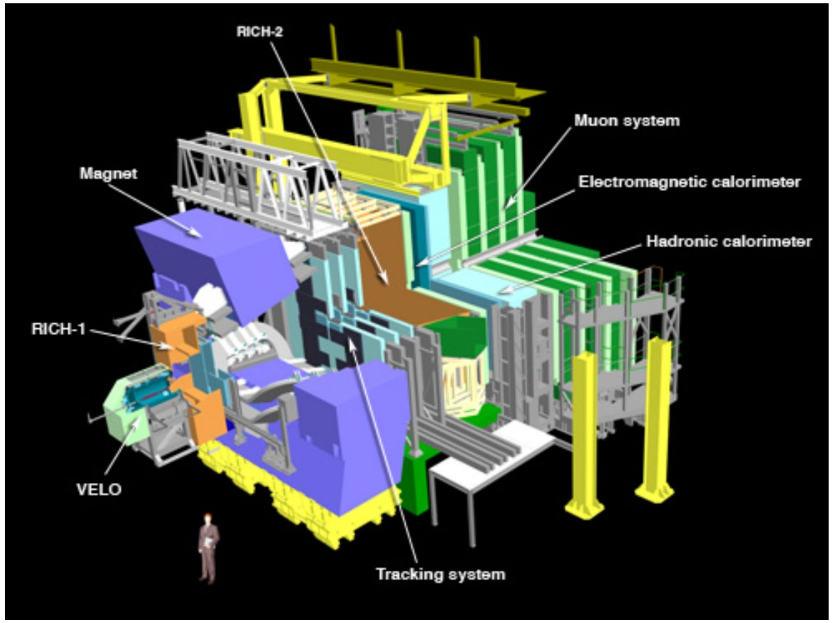

Some things to consider when choosing parts of these for your tera-Z flavour experiment

At much lower energy than tera-Z: about 10 GeV instead of about 90 GeV.

Asymmetric beams so b's tend to go "forward", more towards one side than the other.

Much higher energy, much more intense radiation environment than tera-Z.

Most b's are produced close to the beam line, so built more like a fixed-target experiment than a collider one

Belle-2 specs

What the current best b physics experiment thought was important

Table 1.3: Expected performance of components of the Belle II spectrometer.

Component	Type	Configuration	Readout	Performance
Beam pipe	Beryllium double-wall	Cylindrical, inner radius 10 mm, 10 μm Au, 0.6 mm Be, 1 mm coolant (paraffin), 0.4 mm Be		impact parameter resolution $\sigma_{z_0} \sim 20\ \mu$m (PXD and SVD)
PXD	Silicon pixel (DEPFET)	Sensor size: 15×100 (120) mm^2 pixel size: 50×50 (75) μm^2 2 layers: 8 (12) sensors	10 M	
SVD	Double sided Silicon strip	Sensors: rectangular and trapezoidal Strip pitch: 50(p)/160(n) - 75(p)/240(n) μm 4 layers: 16/30/56/85 sensors	245 k	
CDC	Small cell drift chamber	56 layers, 32 axial, 24 stereo r = 16 - 112 cm - 83 $\leq z \leq$ 159 cm	14 k	$\sigma_{r\phi} = 100\ \mu$m, $\sigma_z = 2$ mm $\sigma_{p_t}/p_t = \sqrt{(0.2\% p_t)^2 + (0.3\%/\beta)^2}$ $\sigma_{p_t}/p_t = \sqrt{(0.1\% p_t)^2 + (0.3\%/\beta)^2}$ (with SVD) $\sigma_{dE/dx} = 5\%$
TOP	RICH with quartz radiator	16 segments in ϕ at $r \sim 120$ cm 275 cm long, 2 cm thick quartz bars with 4x4 channel MCP PMTs	8 k	$N_{p.e.} \sim 20$, $\sigma_t = 40$ ps K/π separation : efficiency $> 99\%$ at $< 0.5\%$ pion fake prob. for $B \to \rho\gamma$ decays
ARICH	RICH with aerogel radiator	4 cm thick focusing radiator and HAPD photodetectors for the forward end-cap	78 k	$N_{p.e.} \sim 13$ K/π separation at 4 GeV/c: efficiency 96% at 1% pion fake prob.
ECL	CsI(Tl) (Towered structure)	Barrel: $r = 125$ - 162 cm End-cap: $z =$ -102 cm and +196 cm	6624 1152 (F) 960 (B)	$\frac{\sigma E}{E} = \frac{0.2\%}{E} \oplus \frac{1.6\%}{\sqrt[4]{E}} \oplus 1.2\%$ $\sigma_{pos} = 0.5\ \text{cm}/\sqrt{E}$ (E in GeV)
KLM	barrel: RPCs	14 layers (5 cm Fe + 4 cm gap) 2 RPCs in each gap	θ: 16 k, ϕ: 16 k	$\Delta\phi = \Delta\theta = 20$ mradian for K_L $\sim 1\ \%$ hadron fake for muons
	end-caps: scintillator strips	14 layers of $(7-10) \times 40$ mm^2 strips read out with WLS and G-APDs	17 k	$\Delta\phi = \Delta\theta = 10$ mradian for K_L $\sigma_p/p = 18\%$ for 1 GeV/c K_L

RICH is ring-imaging Cherenkov detector

Note though this was a much lower energy machine, with beams of differing energies to give the b's a longitudinal boost.

LHCb subdetectors

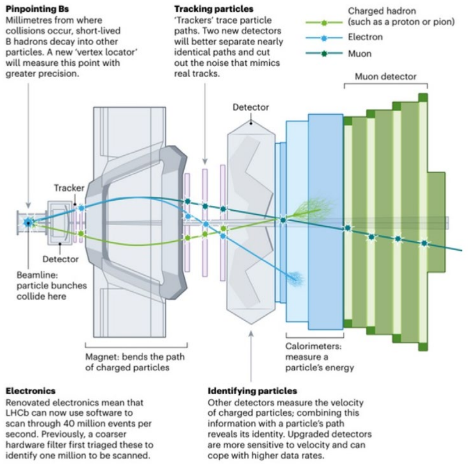

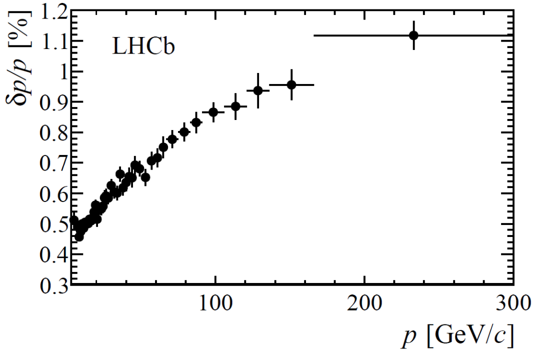

Figure 17: Relative momentum resolution versus momentum for long tracks in data obtained using J/ψ decays.

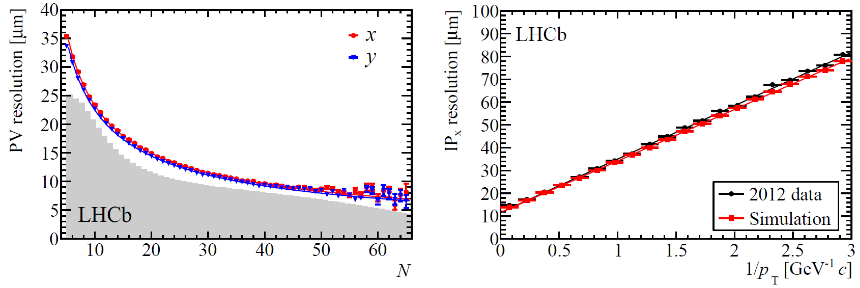

Figure 25: The primary vertex resolution (left), for events with one reconstructed primary vertex, as a function of track multiplicity. The x (red) and y (blue) resolutions are separately shown and the superimposed histogram shows the distribution of number of tracks per reconstructed primary vertex for all events that pass the high level trigger. The impact parameter in x resolution as a function of $1/p_T$ (right). Both plots are made using data collected in 2012.

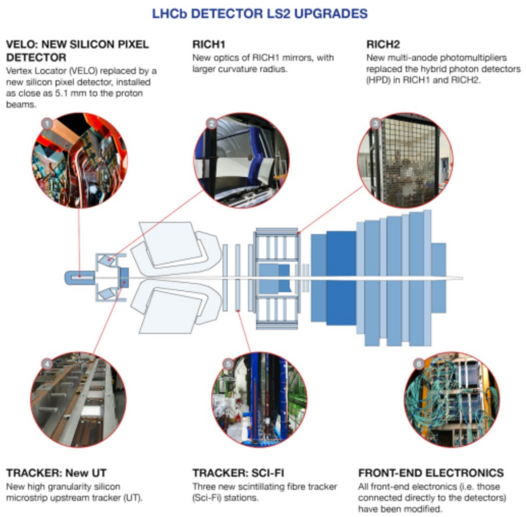

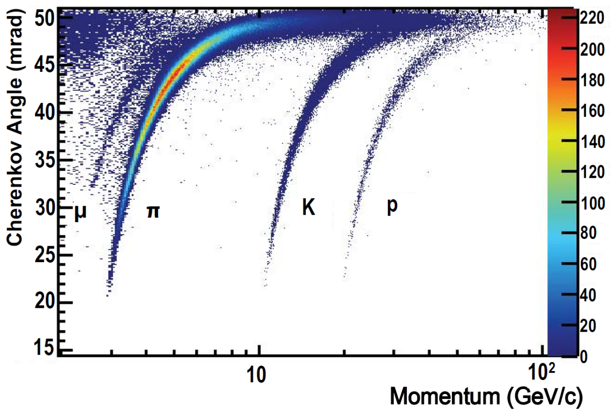

Figure 38: Reconstructed Cherenkov angle for *isolated* tracks, as a function of track momentum in the C_4F_{10} radiator [81]. The Cherenkov bands for muons, pions, kaons and protons are clearly visible.

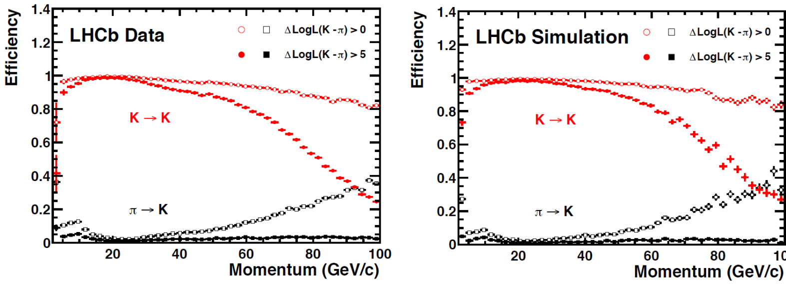

Figure 39: Kaon identification efficiency and pion misidentification rate as measured usi data (left) and from simulation (right) as a function of track momentum [81]. Two differe $\Delta\log\mathcal{L}(K-\pi)$ requirements have been imposed on the samples, resulting in the open and fill marker distributions, respectively.

Specs from recent CEPC paper

https://arxiv.org/abs/2209.14486 Studied $D^0 \rightarrow \pi^+ K^-$ and $\phi \rightarrow K^+ K^-$

- Time of flight resolution of 50 ps for a flight path radius of a bit over 3 meters
- dE/dx resolution of 3% in barrel for charged particles with energy> 2 GeV

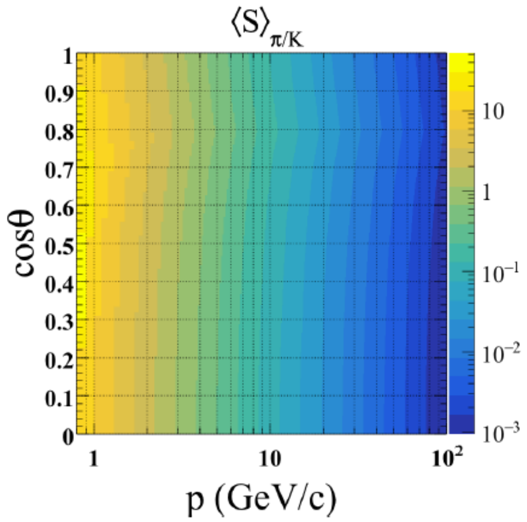

Figure 3: The $K^{\pm}/\pi^{\pm}$ separation power as a function of momentum and cosine polar angle with TOF information.

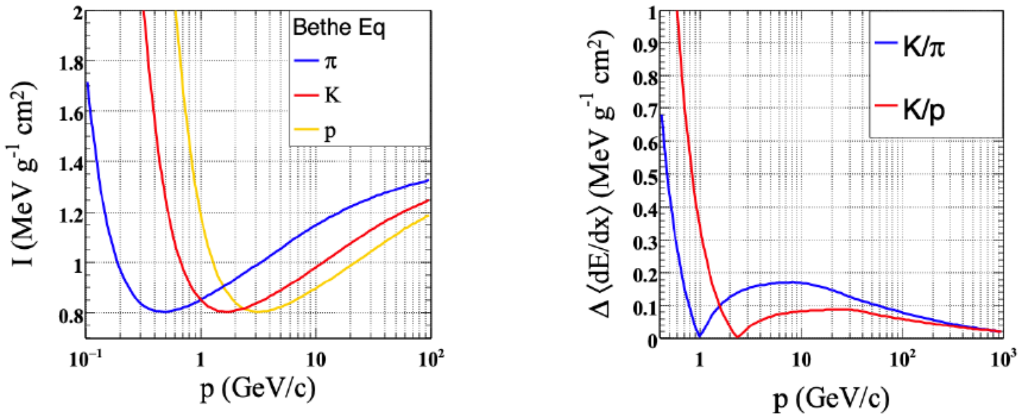

Figure 4: The distribution of I as a function of momentum for $K^{\pm}/\pi^{\pm}/\overset{(-)}{p}$ is shown in the left plot and the absolute difference of I for $K^{\pm}/\pi^{\pm}$ and $K^{\pm}/\overset{(-)}{p}$ is shown in the right plot.

Specs from snowmass report

Report of the Frontier for Rare Processes and Precision Meaurements: arXiv:2210.04765

TABLE II. Detector specifications for representative RPF experiments (medium term goals)

Experimental approach	Technology	Property	Requirement
Quark flavor experiments	Solid State Tracking Detectors	Time stamp Radiation hardness	10-30ps/hit in the silicon pixel vertex detector fluences up to $5 \times 10^{1}6\mathrm{n}_{\mathrm{eq}}/\mathrm{cm}^2$
	Calorimetry	Time stamp resolution	10-30 ps/shower
	Trigger & DAQ	Real time processing Optical links	400-500 TB/sec Radiation-hard, fast, low-power and low-mass
LFV experiments (μ)	Staw Tube Tracker	timing	20 ps/track, low-mass, excellent momentum resolution
	Calorimetry	Energy resolution timing	$< 10\%/\sqrt{E}$, low cost Shower time stamp < 500 ps, dose > 900 KRad
EDMs	Controlled preparation of many coherent particles	coherence times	$\tau \geq 1s$ or $N >> 10^{12}$
	Laser locking, tuning and linewidth narrowing (many narrow-band lasers on target)	tunable narrow band	< 1 MHz, $\lambda = 2002 - 400$nm
Dark Sector (missing energy technique)	E&M calorimetry	Energy resolution	
Dark Sector (Beam Dump experiments)	photosensors	fast-timing photosensors	

So let’s have some fun

Let’s divide into a few small groups. Working together, design a detector. We can then quickly show what we choose. Some slides are included here for some choices you can make based on existing designs (and of course you can always look directly in the reference). Also think about subdetectors in Belle-2 that you may want to add.

Some references

- ILC detector TDR https://linearcollider.org/technical-design-report/ (volume 4 –detectors)
- FCC TDR with detectors https://link.springer.com/article/10.1140/epjst/e2019-900045-4 (chapter 7)
- A recent paper by CEPC on flavor requirements https://arxiv.org/abs/2209.14486
- Description of the Belle-2 detector at SuperKEKB https://arxiv.org/abs/1011.0352 (state of the art b physics experiment. Asymmetric beam energies, so some care needs to be taken when extrapolating to a tera-Z factory)
- Belle-2 upgrade https://arxiv.org/abs/2203.11349
- A calorimeter design with improved electromagnetic resolution https://iopscience.iop.org/article/10.1088/1748-0221/15/11/P11005
- CEPC detectors https://arxiv.org/abs/1811.10545
- IDEA detector https://inspirehep.net/files/49ec726758c422bc454e270a71f6e59f
- LHCb upgrade https://cds.cern.ch/record/1443882/files/LHCB-TDR-012.pdf
- LHCb detector performance https://arxiv.org/abs/1412.6352
- The LHCb detector https://cds.cern.ch/record/1129809?ln=en
- Snowmass report on rare and precision measurements https://arxiv.org/abs/2210.04765
- Detectors for extreme luminosity: belle II https://www.phys.hawaii.edu/~teb/BelleII_NIM_special.pdf

trackers

ILD
- TPC/Silicon
- B field 3.5 T
- Radius 3.4 m

SiD
- All silicon tracking
- B field 5.0 T
- Radius 1.2 m

IDEA
- Drift chamber/ silicon
- B field 2 T
- Radius 2.1 m

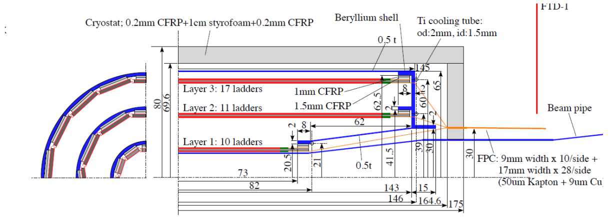

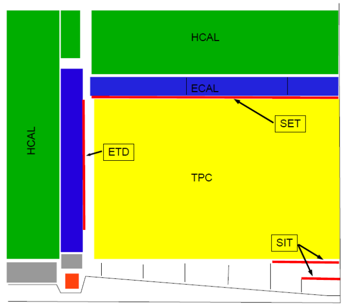

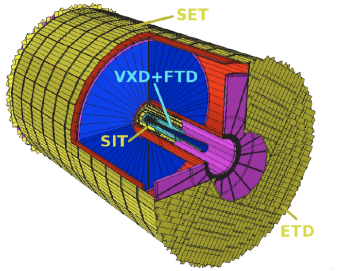

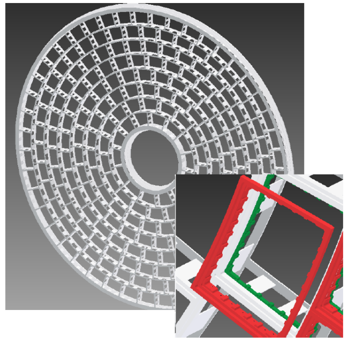

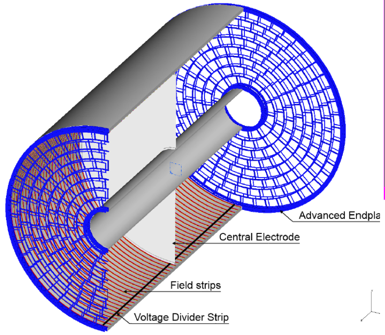

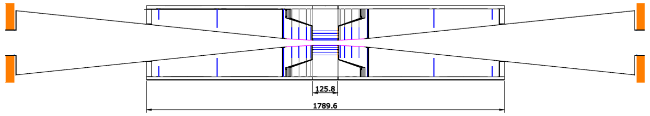

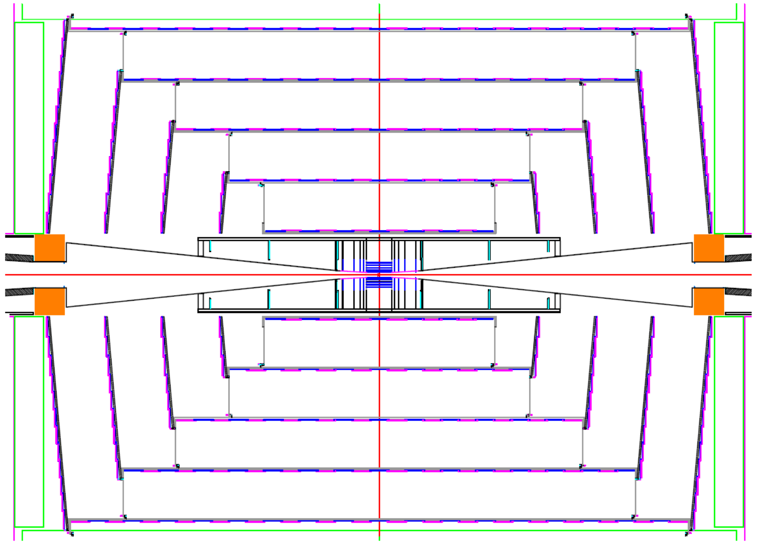

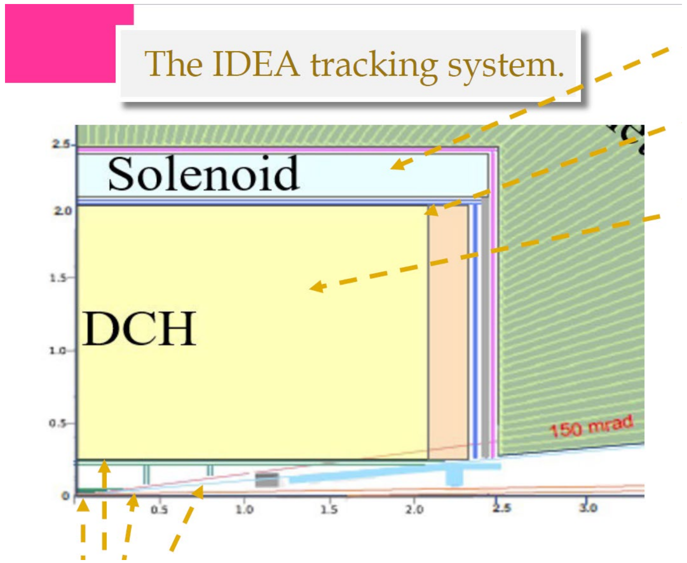

SiD tracker performance

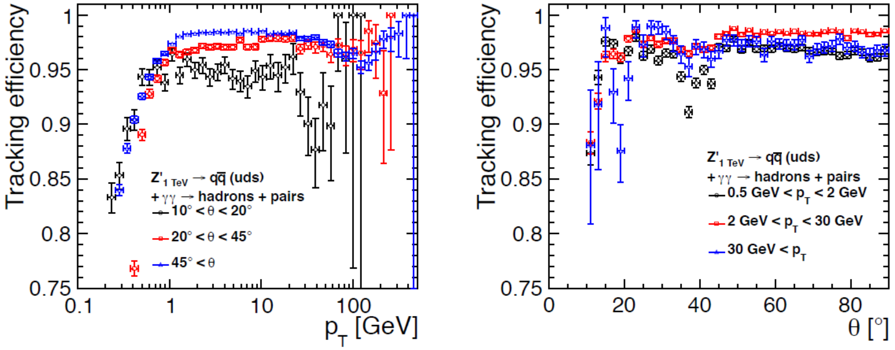

Figure II-3.9 Normalised transverse momentum resolution for single-muon events in SIDLOI3 as function of momentum. The dashed lines indicate a fit to the parametrisation given in Equation II-3.1.

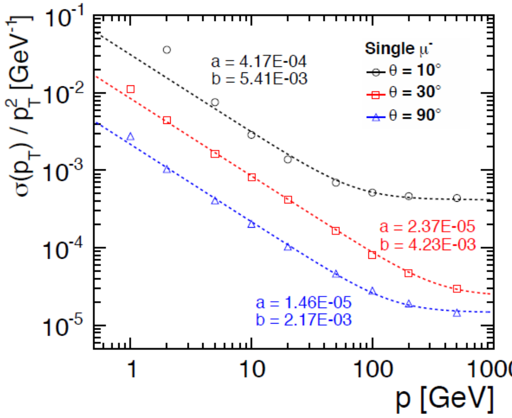

Figure II-3.10 Impact parameter resolution $\sigma(d_0)$ (left) and $\sigma(z_0)$ (right) for single muon events in SIDLOI3 as function of the polar angle θ.

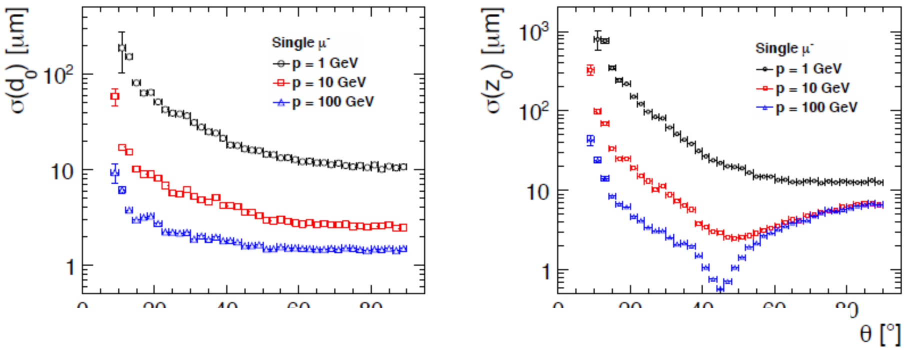

Figure II-10.4 The nuclear interaction lengths of SIDLOI3 (left) and the radiation lengths of SIDLOI3 tracking system (right) as a function of the polar angle θ.

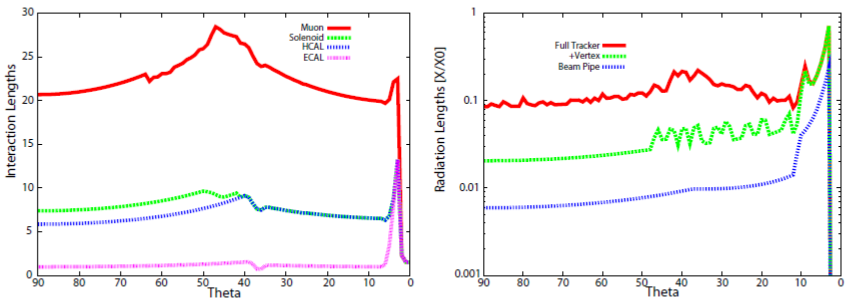

Figure II-10.9 Mis-identification efficiency of light quark jets (red points) and charm jets (green points) as beauty jets versus beauty identification efficiency in di-jets at $\sqrt{s} = 91$ GeV. The performance is shown without (left) and with background from $\gamma\gamma \rightarrow$ hadrons events and incoherent pairs (right).

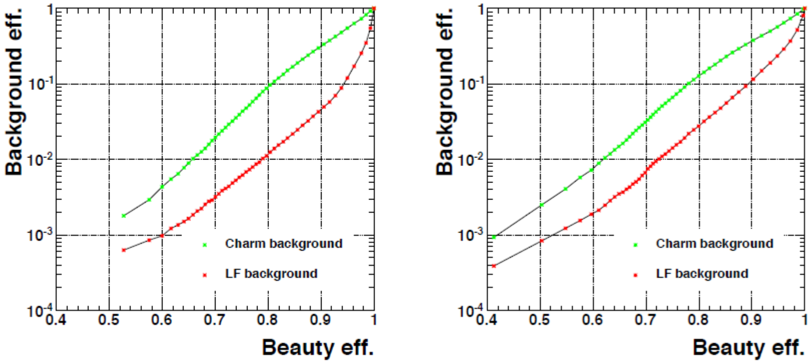

(a) without $\gamma\gamma \rightarrow$ hadrons (b) with $\gamma\gamma \rightarrow$ hadrons

Figure II-10.10 Position of the reconstructed primary vertex (left) and resolution of the primary vertex position as a function of the number of tracks originating from that vertex (right).

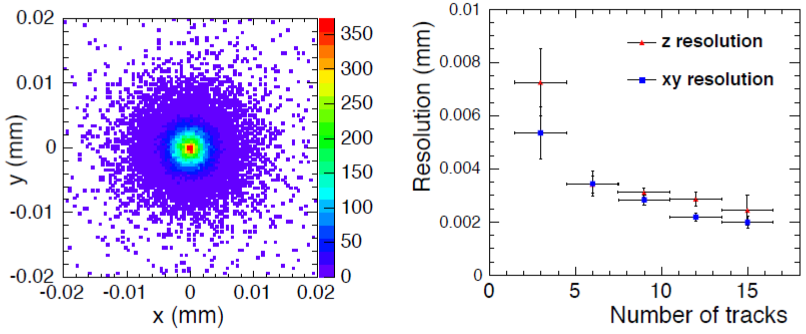

FUTURE CIRCULAR COLLIDER

ILD tracker performance

Table III-2.4
Performance and design parameters for the TPC with standard electronics and pad readout.

Parameter	
Geometrical parameters	r_{in} 329 mm, r_{out} 1808 mm, z ± 2350 mm
Solid angle coverage	up to $\cos\theta \simeq 0.98$ (10 pad rows)
TPC material budget	$\simeq 0.05\ X_0$ including outer fieldcage in r
	$< 0.25\ X_0$ for readout endcaps in z
Number of pads/timebuckets	$\simeq 1\text{-}2 \times 10^6/1000$ per endcap
Pad pitch/ no.padrows	$\simeq 1 \times 6\ \text{mm}^2$ for 220 padrows
σ_{point} in $r\phi$	$\simeq 60\ \mu m$ for zero drift, $< 100\ \mu m$ overall
σ_{point} in rz	$\simeq 0.4 - 1.4$ mm (for zero – full drift)
2-hit resolution in $r\phi$	$\simeq 2$ mm
2-hit resolution in rz	$\simeq 6$ mm
dE/dx resolution	$\simeq 5$ %
Momentum resolution at B=3.5 T	$\delta(1/p_t) \simeq 10^{-4}$/GeV/c (TPC only)

Figure III-1.4
Left: Average total radiation length of the material in the tracking detectors as a function of polar angle. Right: Total interaction length in the detector, up to the end of the calorimeter system, and including the coil of the detector.

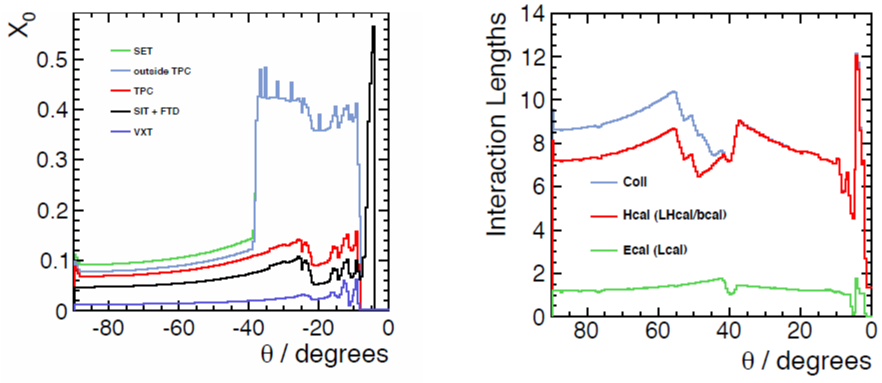

Figure III-6.2
Tracking Efficiency for $t\bar{t} \to 6$ jets at 500GeV and 1 TeV plotted against (left) momentum and (right) $\cos\theta$.

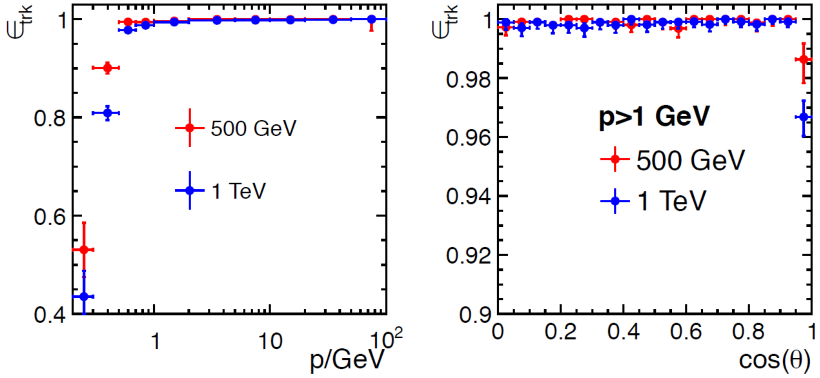

Figure III-2.1
Impact parameter resolution of the ILD vertex detector for two different particle production angles (20° and 85°), assuming the baseline point resolution given in Table III-2.1 for the CMOS option (solid line), and the FPCCD option (dotted line). The curves with long dashes show the performance goal.

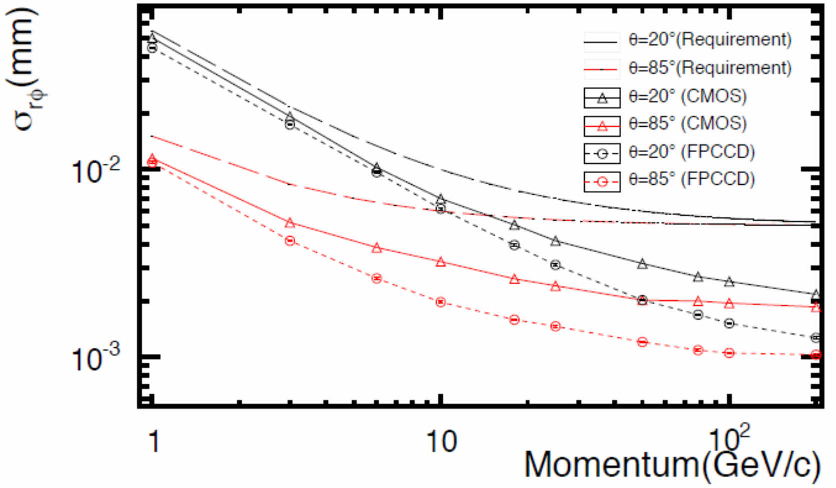

Fi
Left: Momentum resolution as a function of the transverse momentum of particles, for tracks with different polar angles. Also shown is the theoretical expectation. Right: Flavour tagging performance for $Z \to q\bar{q}$ samples at different energies.

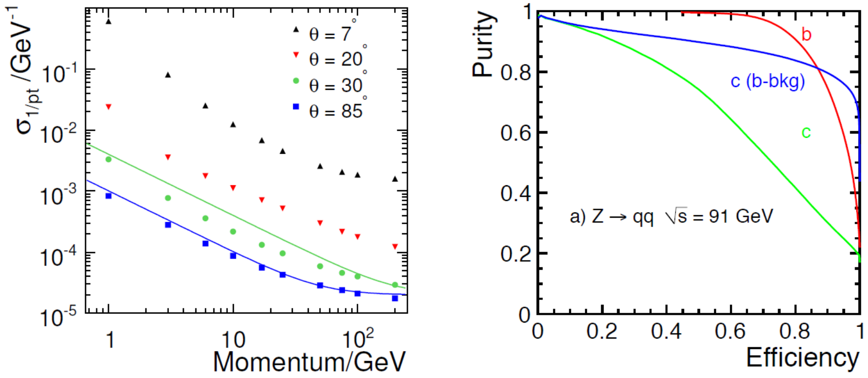

IDEA

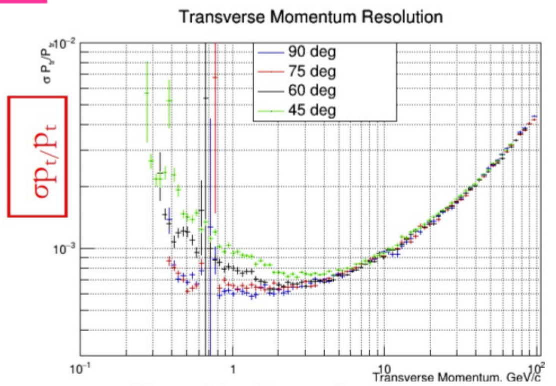

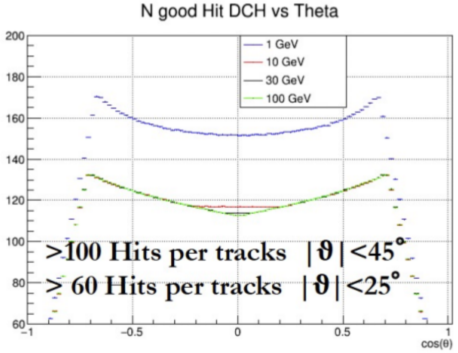

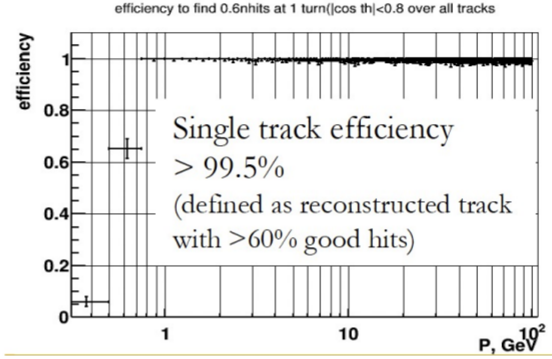

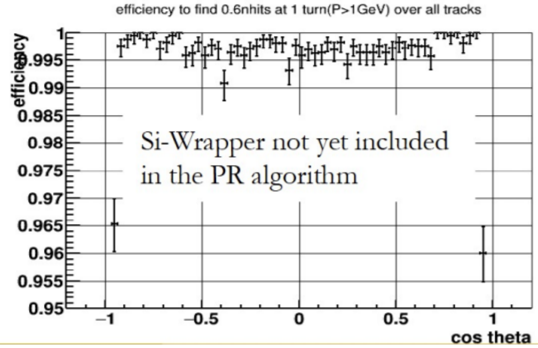

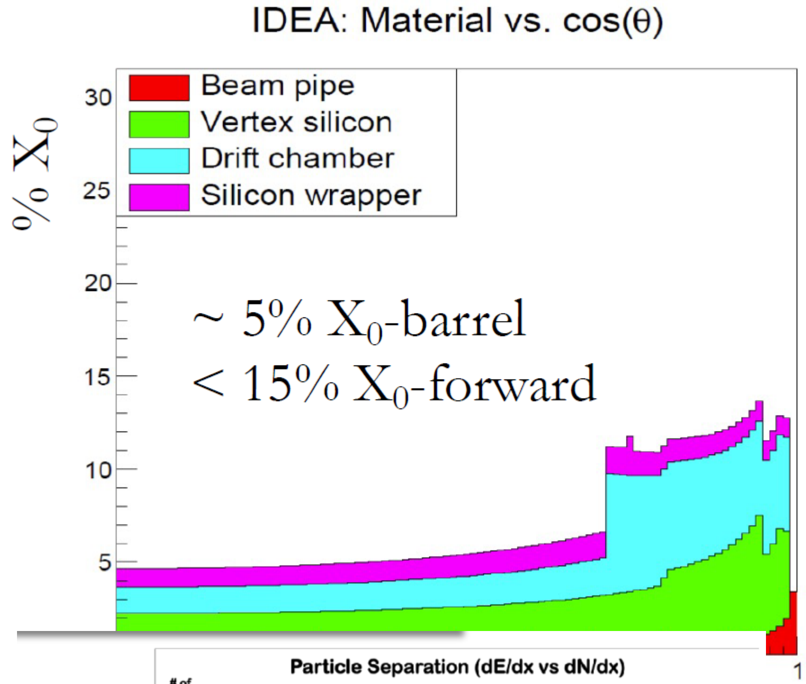

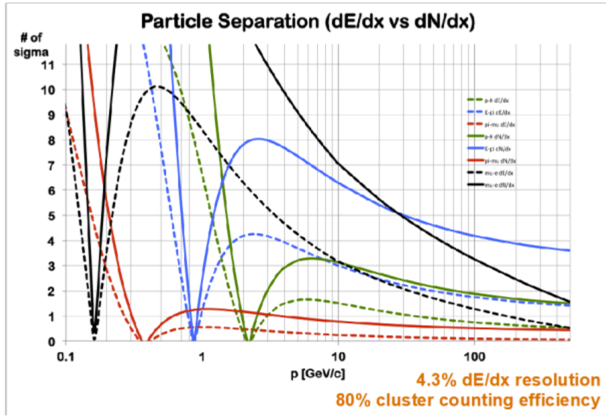

- Cluster Counting/Timing in DCH for good P.Id. Performance
- Expected excellent K/π separation over the entire range except 0.85<p<1.05 GeV (blue lines).
- Could recover with timing layer.

calorimeters

ILD (and most other designs)

- High granularity

Figure III-3.3
Cross sections through electromagnetic calorimeter layers for the silicon option (left) and for the scintillator option (right).

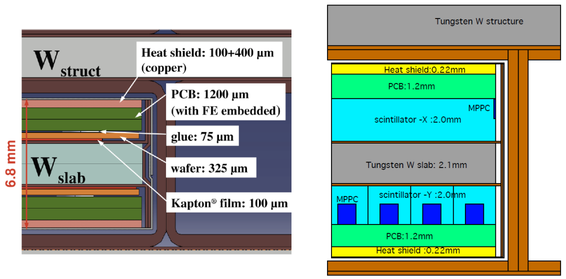

Figure III-3.14
Arrangement of AH-CAL layers with electronic components (left), cross section of an active layer (right).

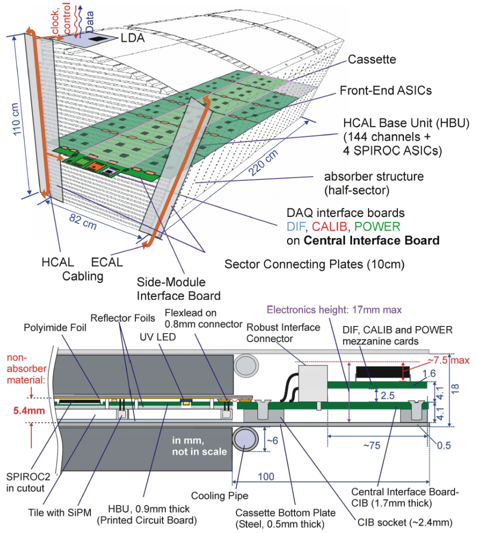

IDEA

- Dual readout fiber

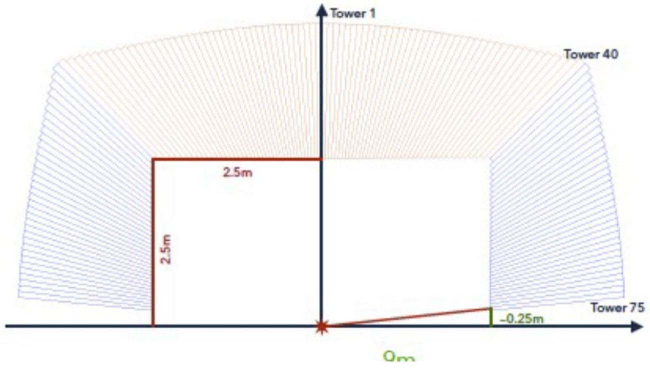

IDEA+crystal ECAL

- Dual readout crystal ecal
- Dual readout fiber hcal
- CMS-barrel like crystal timing detector in front of ecal

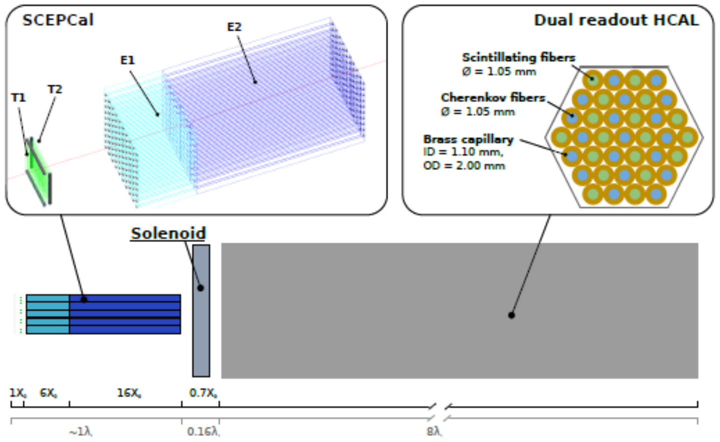

ILD calorimeter

Figure III-1.6
Fractional jet energy resolution plotted against $|\cos\theta|$ where theta is the polar angle of the thrust axis of the event.

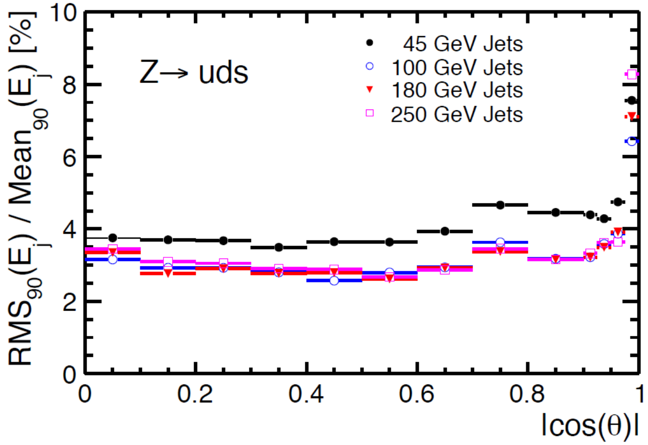

Figure III-3.18
Reconstructed energy (left) and energy resolution (right) of the AHCAL for pion showers starting in the first five calorimeter layers. Shown are results obtained with a simple energy sum and with a local and a global software compensation (SC) technique, respectively. The green band indicates the systematic error of the calibration, and is shown around the results with with initial energy reconstruction. Figure taken from [315].

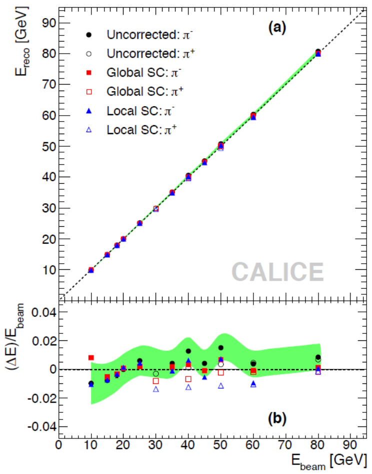

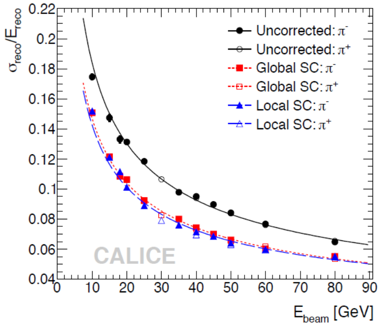

fit results		
	stochastic	constant
initial	57.6%	1.6%
global SC	45.8%	1.6%
local SC	44.3%	1.8%

Figure III-3.8
Jet energy resolution in $q\bar{q}(q = uds)$ events at different centre of mass energies, using a hybrid ECAL with silicon (Si) and scintillator (Sc) layers. The jet energy resolution is shown as a function of the fraction of scintillator layers in the ECAL, (Sc/(Sc+Si)). The total number of ECAL layers (Sc+Si) is 28.

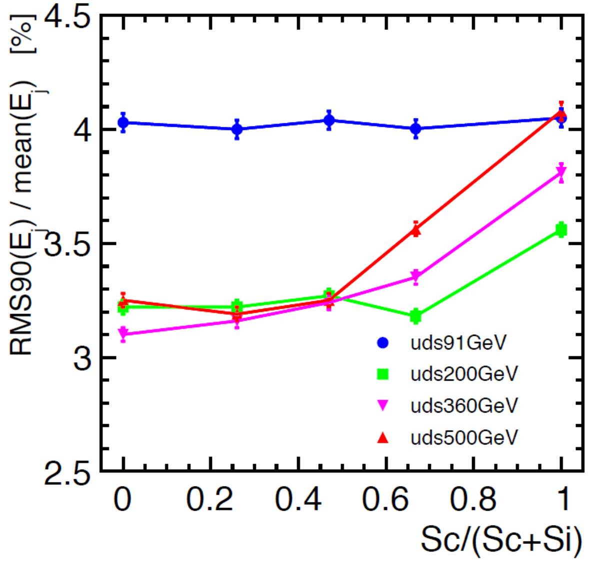

IDEA

Geant4 indications on the expected performance (selected results):

- 10% – 15 % / $\sqrt{E}$ EM energy resolution.
- 25% – 30 % / $\sqrt{E}$ energy resolution for single hadrons (including neutral hadrons).
- energy resolution for jets at 50 GeV.
- Sub-percent linearity in the FCCee energy ranges for e^-/γ, hadrons and jets.

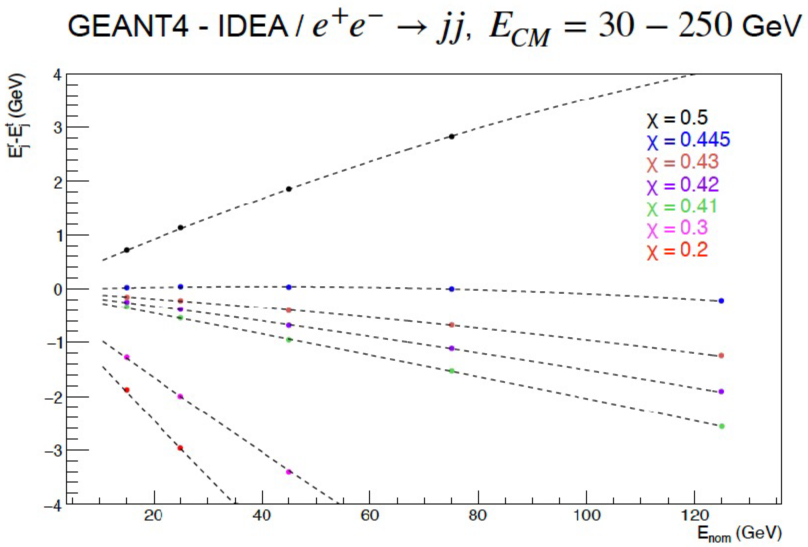

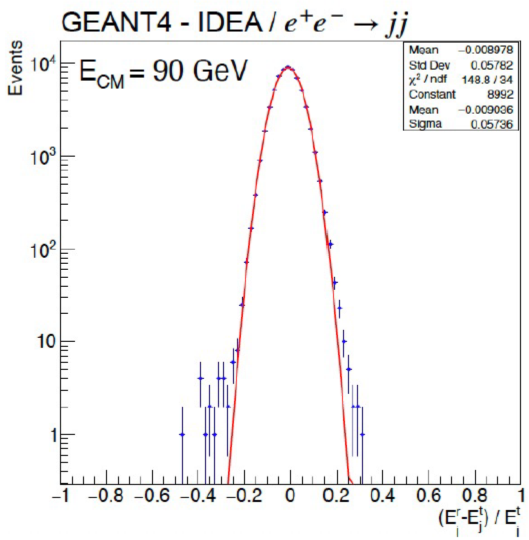

IDEA plus crystal ECAL

https://arxiv.org/abs/2202.01474

https://iopscience.iop.org/article/10.1088/1748-0221/15/11/P11005

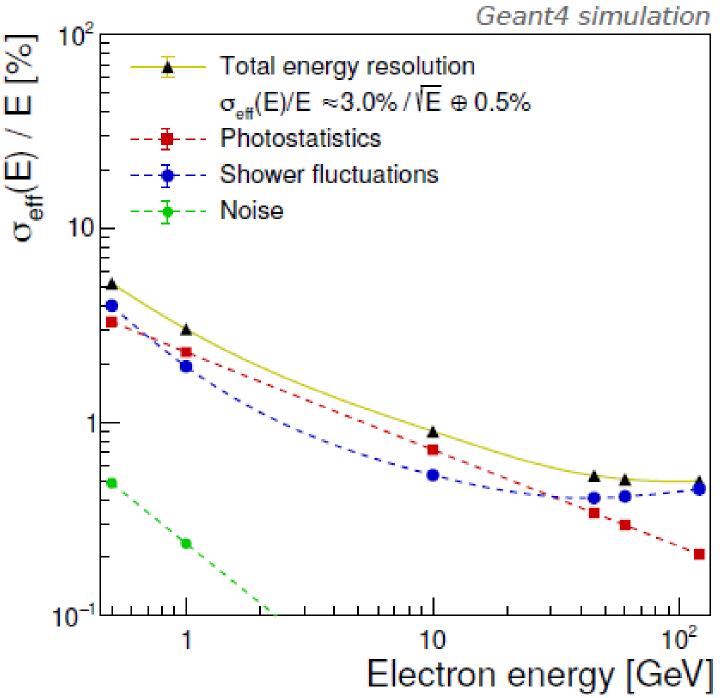

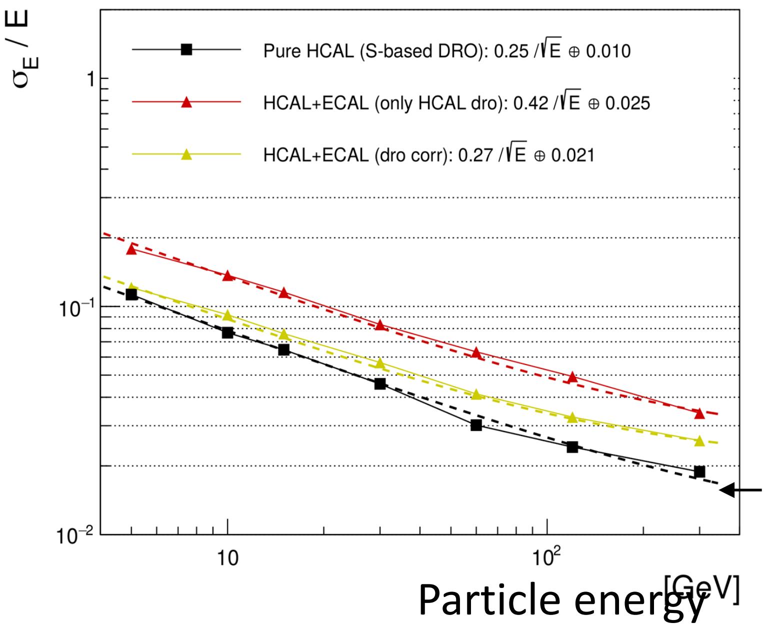

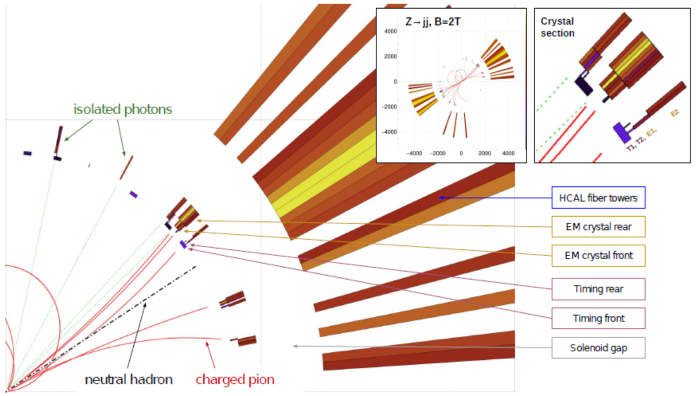

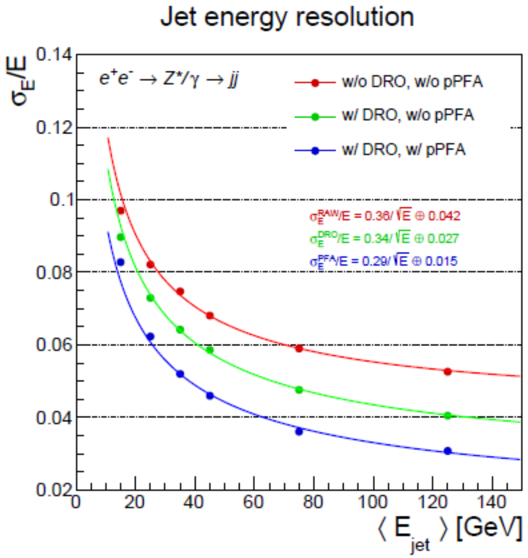

Flavor specific subdectors (Belle-2)

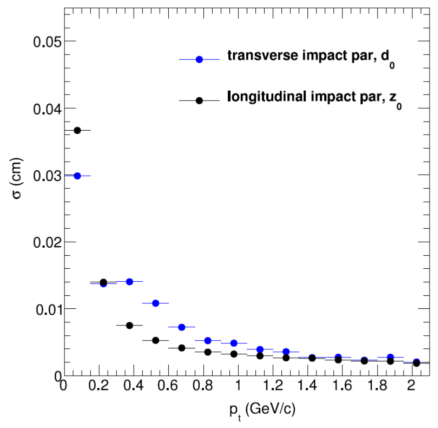

Fig. 27. Transverse and longitudinal IP resolution as a function of transverse momentum as determined on simulated data.

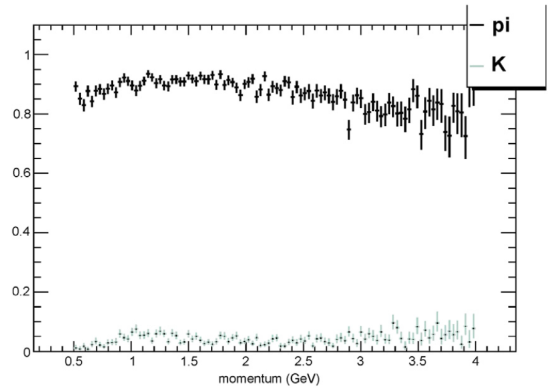

Fig. 28. Pion identification efficiency and kaon mis-identification rate as a function of momentum, determined on simulated event samples.

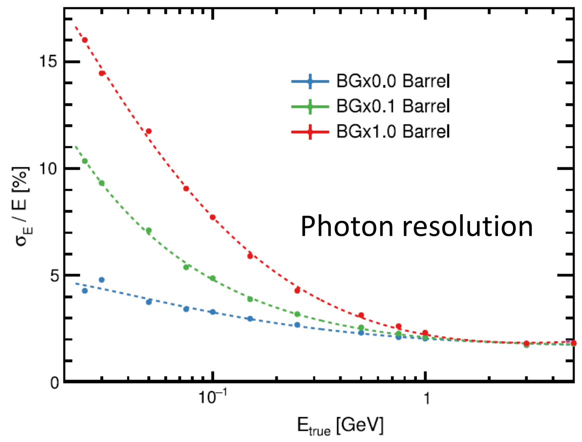

Fig. 29. Belle II ECL energy resolution, simulated data with and without beam background.

Table 5
Summary of detector performance.

Measurement	Belle	Belle II
B Vertex Reconstruction (typical)	$\sigma_z = 61\,\mu\text{m}$	$\sigma_z = 26\,\mu\text{m}$
Tracking	$\sigma_{p_t}/p_t = 0.0019 p_t\ [\text{GeV}/c] \oplus 0.0030/\beta$	$\sigma_{p_t}/p_t = 0.0011 p_t\ [\text{GeV}/c] \oplus 0.0025/\beta$
$K\pi$ ID	Kaon efficiency $\epsilon_K \simeq 0.85$ with pion fake rate $\epsilon_\pi \simeq 0.10$ for $p = 2\,\text{GeV}/c$	$\epsilon_K \simeq 0.90$ with $\epsilon_\pi \simeq 0.04$ for $p = 2\,\text{GeV}/c$
Calorimetry	$\frac{\sigma_E}{E} = \frac{0.066\%}{E} \oplus \frac{0.81\%}{\sqrt[4]{E}} \oplus 1.34\%$	$\frac{\sigma_E}{E}$ = 7.7% at 0.1 GeV, 2.25% at 1 GeV (Fig. 29)
Muon ID	Muon efficiency $\epsilon_\mu \simeq 0.90$ with fake rate $\epsilon \simeq 0.02$ for $p_t > 0.8\,\text{GeV}/c$ tracks	$\epsilon_\mu = 0.92 - 0.98$ with $\epsilon = 0.02 - 0.06$ for $p > 1\,\text{GeV}/c$
L1 Trigger	500 Hz typical average, Efficiency for hadronic events $\epsilon_{\text{hadron}} \simeq 1$	30 kHz max. average rate, $\epsilon_{\text{hadron}} \simeq 1$
DAQ	~5% dead time at 500 Hz L1 rate	<3% dead time at 30 kHz L1 rate

SiD costs

Table II-12.2
Summary of Costs per Subsystem.

SiD

	M&S Base (M US-$)	M&S Contingency (M US-$)	Engineering (MY)	Technical (MY)	Admin (MY)
Beamline Systems	3.7	1.4	4.0	10.0	
VXD	2.8	2.0	8.0	13.2	
Tracker	18.5	7.0	24.0	53.2	
ECAL	104.8	47.1	13.0	288.0	
HCAL	51.2	23.6	13.0	28.1	
Muon System	8.3	3.0	5.0	22.1	
Electronics	4.9	1.6	44.1	41.7	
Magnet	115.7	39.7	28.3	11.8	
Installation	4.1	1.1	4.5	46.0	
Management	0.9	0.2	42.0	18.0	30.0
	314.9	126.7	186.0	532.1	30.0

ILD costs

The total cost of the ILD detector is summarised in Table III-7.7. The distribution of the costs

Table III-7.7
Summary table of the cost estimate of the ILD detector. Depending on the options used the cost range is between 336 Mio ILCU and 421 Mio ILCU.

System	Option	Cost [MILCU]	Mean Cost [MILCU]
Vertex			3.4
Silicon tracking	inner	2.3	2.3
Silicon tracking	outer	21.0	21.0
TPC		35.9	35.9
ECAL			116.9
	SiECAL	157.7	
	ScECAL	74.0	
HCAL			44.9
	AHCAL	44.9	
	SDHCAL	44.8	
FCAL		8.1	8.1
Muon		6.5	6.5
Coil, incl anciliaries		38.0	38.0
Yoke		95.0	95.0
Beamtube		0.5	0.5
Global DAQ		1.1	1.1
Integration		1.5	1.5
Global Transportation		12.0	12.0
Sum ILD			391.8

ILD

Idea + crystal ecal cost

Since homogeneous calorimeters tend to be expensive, the authors of Ref. [13] have done a cost estimate for an SCEPCal-type calorimeter system, to examine the financial feasibility. Following the general lines of the IDEA detector design, the costing assumes a $PbWO_4$ barrel EM calorimeter with an inner radius of 1.0 m, and a length of 4.7 m. The endcap calorimeter has an inner radius of 0.3 m. The crystals are $1\times1\times20\,\mathrm{cm}^3$ and have two depth segments. The first depth segment has one SiPM while the second has two (as dual readout is only done in the second segment). The total number of barrel crystal towers is 429,300 with $3 \times 429,300$ SiPMs. For the endcap, the number of crystal towers is 174,000, with $3 \times 174,000$ SiPMs. At a cost of $8/cc (an estimate from the Shanghai Institute of Ceramics), the total cost of the crystals is 100 M$. Assuming a cost per

SiPM of $5, and a cost per channel of $4.5 for electronics, power, and monitoring, the per channel cost is $9.5, corresponding to a total electronics cost of 17 M$. The total estimated cost of the EM calorimeter is then about 120 M$. Scaling the cost to the case of BGO, with a crystal volume 23% greater and a cost per cc 14% less according to the SIC cost estimates, and larger crystals with an 11% larger transverse size to match the Molière radius, the overall of the EM calorimeter would be essentially the same, within several percent. The cost for the spaghetti fiber HCAL, when using 2.5mm outer diameter brass tubes, as estimated by the IDEA collaboration, is 35 M$. The EM + HCAL cost overall is thus not unaffordable.